Article

Not peer-reviewed version

Designing Microfluidic PCR Chip Device Using CFD Software for the Detection of Malaria

Meynard R. Austria *, Jon Patrick T. Garcia *, Lemmuel L. Tayo *, Alvin R. Caparanga *, Bonifacio Jr T. Doma *

Posted Date: 10 August 2023

doi: 10.20944/preprints202305.1033.v2

Keywords: polymerase chain reaction (PCR); Computational Fluid Dynamics (CFD); Plasmodium falciparum; microfluidic chip design

Article

Designing Microfluidic PCR Chip Device Using CFD Software for the Detection of Malaria

Meynard Austria [1], Jon Patrick Garcia [1], Alvin Caparanga [1], Lemmuel Tayo [1,2] and Bonifacio Doma [1,2]

[1] School of Chemical, Biological, and Materials Engineering and Sciences, Mapúa University, Manila 1002, Philippines

[2] Department of Biology, School of Medicine and Health Sciences, Mapúa University, Makati 1200, Philippines

Abstract: Polymerase chain reaction (PCR) technique is one of the molecular methods in amplifying DNA for the detection of malaria. However, the limitations of PCR especially when used for routine clinical practice can hamper its sensitivity and specificity. With that, this study focuses on designing a microfluidic device that will mimic the function of a conventional genus-specific PCR based on 18S rRNA gene to detect malaria parasites (*Plasmodium falciparum*) at low grade parasitemia. The design was drawn and simulated using ANSYS 14.5 Computational Fluid Dynamics (CFD). The simulation shows that adding loops to the design increases its relative deviation but to a minimal extent as compared to having only a straight path design, which indicates that looping is acceptable in designing a microfluidic device to minimize chip length. Also, increasing the cross-sectional area of the fluid path decreases the efficiency of the design, thus, the design with a relatively smaller cross-sectional area is favored. And lastly, among the three materials utilized, the chip made of polypropylene is the most efficient with a relative deviation of 0.94 as compared to polycarbonate and polydimethylsiloxane which have relative deviations of 2.78 and 1.92, respectively.

Keywords: polymerase chain reaction (PCR); Computational Fluid Dynamics (CFD); *Plasmodium falciparum;* microfluidic chip design

1. Introduction

Malaria is a disease caused by Plasmodium parasites of different species such as *Plasmodium falciparum, Plasmodium vivax, Plasmodium malariae,* and *Plasmodium ovale.* Among these species, *Plasmodium falciparum* and *Plasmodium vivax* are the most common and *Plasmodium falciparum* is the deadliest [1]. These parasites are transmitted to people through the bites of infected mosquitoes, and malaria is highly widespread in tropical and subtropical countries [2]. In 2021, based on the World Health Organization, an estimated 247 million malaria cases were recorded among the 84 malaria endemic countries, with the African region accounting around 95% of the total cases globally [3]. Aside from that, 13.4 million cases between the years 2019 and 2021 were aggravated by the ramifications brought by the COVID-19 pandemic [4]. Individuals from continuous transmission areas may, after several malaria infections, develop the premonition state which is characterized by an immune response that is able to control the parasitemia but unlikely to purge all the circulating parasites [5]. As a result, those individuals can stay asymptomatic and act as a parasitic reservoir since such infected blood is now able to infect mosquito vectors, and with that, these may reintroduce malaria into other regions [6].

The foundation of PCR is the enzymatic amplification of specific DNA sequences. It makes use of the capacity to synthesize DNA strands of the heat-resistant Taq DNA polymerase [7]. The specific DNA region of the malaria parasite is amplified exponentially, producing millions of copies that are readily detectable. Targeted DNA sections within the parasite's genome are used in PCR to identify malaria parasites. To enable the identification of different strains, these areas must be retained across different Plasmodium species [8]. Short DNA sequences called primers are created to selectively attach to the DNA of the parasite and flank the target region [9]. So in order to detect malaria with

 doi:10.20944/preprints202305.1033.v2

high sensitivity and specificity, primer design is essential. The designed nucleotides, Taq polymerase enzyme, and the extracted DNA are combined. Denaturation, annealing, and extension cycles are repeatedly performed during thermal cycling [10]. Exponential amplification occurs as a result of each cycle doubling the size of the targeted DNA region. Several techniques can be used to determine whether malaria parasite DNA is present following PCR amplification [11]. Gel electrophoresis is a popular technique that uses an electric field to separate the amplified DNA fragments according to size [12]. DNA-staining dyes can be used to see the resultant bands. As an alternative, real-time PCR can be done to analyze DNA amplification quantitatively in real-time [13]. The fluorescence signal for each cycle is evaluated using fluorescent probes or DNA-binding dyes. The amount of DNA amplification coincides with the fluorescence level. PCR has many benefits for finding malaria parasites. It has a great sensitivity and can find even a single parasite DNA molecule in a sample [14]. Additionally, it offers great specificity, reducing false-positive outcomes. PCR can identify drug-resistant strains and distinguish between several Plasmodium species [15]. However, PCR is difficult to use in situations where resources are limited because it calls for specialized lab equipment and skilled technicians [16].

Malaria is commonly diagnosed by microscopic examination using Giemsa-stained TBS which is known as the gold standard method for malaria diagnosis, but this technique is not the best choice for low level parasitemia and for mixed infections [17,18]. However, in some endemic areas, asymptomatic infections are not usually detectable by microscopic examination. This limitation impacts malaria control and screening of blood samples [19]. Therefore, there is a need for a rapid and accurate diagnosis for effective treatment and control of malaria. It is necessary to develop diagnostic techniques with a high degree of sensitivity and specificity for detecting malaria among environments with relatively low parasite rates and among individuals who are asymptomatic to such disease [20]. Polymerase chain reaction (PCR) assay is found to be one of the most sensitive and specific methods in the detection of malaria parasites. A study was conducted to optimize a faster and cheaper real-time genus-specific PCR based on 18S rRNA gene to detect malaria parasites at low grade parasitemia leading to a threshold sensitivity of 0.2 parasites per 1 μL [21]. However, the time interval concerning the collection and transportation of samples, and the processing and dissemination of results limit the usefulness of PCR in routine clinical practice. Besides that, in most areas with malaria transmission, factors such as limited financial resources, persistent subclinical parasitemia, and inadequate laboratory infrastructures in the poor, remote rural areas impede PCR as a diagnostic method [22,23]. These factors reason for the need to create a microfluidic device that is portable, economical, and accessible but still functional like how the conventional PCR is.

This concept of miniaturizing PCR aims to speed up the process of conventional PCR by reducing the overall sample volume and consumption of reagents, lessening the cost of fabrication, and developing a field-based real-time PCR platform that is capable of completely conducting analyses from raw samples into promising results that will ensure a better method of diagnosing malaria. With the growing interest in developing in-field diagnostic devices that could be used by non-technical personnel involved, this study would surely provide the necessary preliminary data of innovating a device that can aid in the prevalence of malaria in the world. Because of that, a real-time PCR-based microfluidics platform that integrates and miniaturizes DNA purification, amplification, and detection is being introduced for in-field detection. The purpose of this study is to design and simulate a microfluidic PCR chip device which can specifically detect *Plasmodium falciparum* DNA fragment amplification using the software ANSYS 14.5 Computational Fluid Dynamics (CFD). The design is based on the real-time PCR amplification setting for conventional genus-specific PCR targeted on 18S rRNA gene to detect malaria parasites (*Plasmodium falciparum*). The fluid property used in the simulation is based on the solvent property of water (see S3). Different types of materials, that is, polypropylene, polycarbonate, and polydimethylsiloxane, were evaluated and certain design considerations such as the effects of looping and increasing the cross-sectional area were analyzed. After simulating various models and conducting the necessary tests, this intends to determine from the results the most appropriate design that will help in pre-selecting the materials and planning the

Preprints (www.preprints.org) | NOT PEER-REVIEWED | Posted: 10 August 2023 doi:10.20944/preprints202305.1033.v2

optimum parameters needed to consider before fabricating the microfluidic PCR chip device for actual use.

2. Materials and Methods

The design was based on the DNA amplification procedure for conventional genus- specific PCR whose target is the 18S rRNA gene in detecting malaria parasites (*Plasmodium falciparum*) at low grade parasitemia. The design requires 25µL of PCR mix and 5µL of DNA sample. The total volume of 30µL then proceeds the annealing, extension, and denaturation processes specified at various temperatures to determine which conditions would the device be most efficient to use (see S1 and S2).

Moreover, three polymers were tested to determine which material best suits the design for fabricating the microfluidic PCR chip. Table 1 lists the thermal properties of the polymeric materials utilized in the design.

Table 1. The types of polymeric material with their corresponding thermal properties used in designing the microfluidic PCR chip.

Material Property	Unit	PP[a],[24]	PC[b],[25]	PDMS[c],[26]
Melting Point	K	432.15	428.15	408.15
Thermal Conductivity	$\frac{W}{m \cdot K}$	0.8	0.24	0.15
Specific Heat	$\frac{kJ}{kg \cdot K}$	1.8	1.2	1.46
Density	$\frac{kg}{m^3}$	920	1200	970

[a] *Polypropylene*
[b] *Polycarbonate*
[c] *Polydimethylsiloxane*

The first part of the simulation was intended to determine the effects of looping on the temperature of the fluid inside the device. Aside from that, this also aimed to assess the influence of looping to the efficiency of the design by calculating their respective relative deviation and average square of difference based on a set temperature of 58°C. Three variations were tested: a design with no loops, one loop, and two loops of the same linear path lengths were drawn. The dimensions of which are shown in Table 2.

Table 2. The dimensions of the three designs utilized in the simulation.

	Total Length Calculation			
Design	**Radius (mm)**	**Circumference (mm)**	**Length (mm)**	**Total Length (mm)**
No Loops[a]	-	-	30	30
One Loop	0.25	1.570796327	14	30
Two Loops	0.25	1.570796327	27	30

[a] *The design is characterized as having only a straight path line.*

The proposed microfluidic PCR chip was modeled using ANSYS 14.5 CFD with the following dimensions: the microfluidic chip with length of 73mm and width of 45.5mm, denaturation with length of 15mm and width of 45.5mm, annealing with length of 15mm and width of 45.5mm, extension with length of 10mm and width of 45.5mm, and the spaces with length of 2mm.

The other parameters considered in designing the microfluidic PCR chip are listed in Table 3. Moreover, Figure 1 shows the 44-cycle microfluidic PCR chip and the 2-cycle microfluidic PCR chip utilized in testing the design.

Preprints (www.preprints.org) | NOT PEER-REVIEWED | Posted: 10 August 2023 doi:10.20944/preprints202305.1033.v2

Table 3. Other parameters considered in the design of the microfluidic PCR chip.

Region	Residence Time (s)	Length (μm)	Passes	Volume	Volumetric Flowrate	Speed (μm/s)
Annealing (58°C)	15	15000	1.5	2.94E+09	1.96E+08	1500
Extension (72°C)	20	10000	3	3.92E+09	1.96E+08	1500
Denaturation (95°C)	10	15000	1	1.96E+09	1.96E+08	1500
Spaces	5.3	8000		1.05E+09	1.96E+08	1500
Total	153	75500	3	9.87E+09		

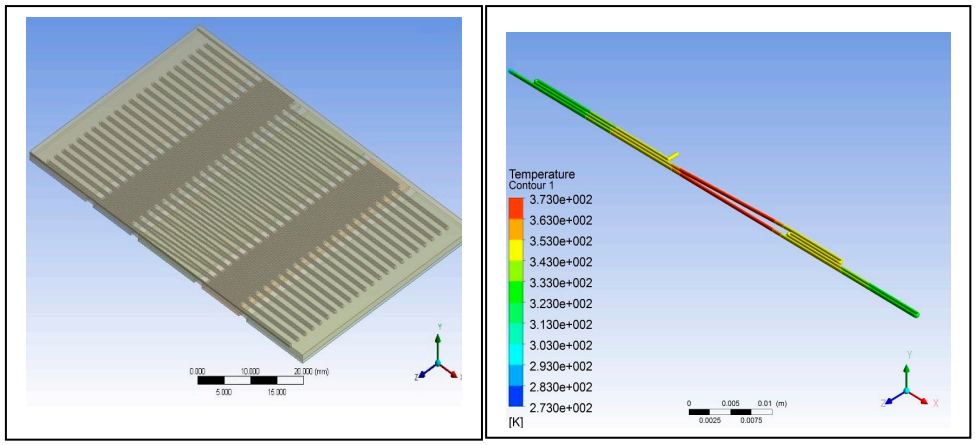

Figure 1. Using ANSYS 14.5 Computational Fluid Dynamics (CFD), the microfluidic PCR chip was modeled to evaluate which design would be best utilized in fabricating the device for actual use. The number of cycles must be specified since this also alters the functionality of the microfluidic PCR chip in detecting malaria. A visual comparison is shown above: (**a**) 44-cycle microfluidic PCR chip design; (**b**) 2-cycle microfluidic PCR chip design.

Different polymeric materials such as polypropylene, polycarbonate, and polydimethylsiloxane were used as the microfluidic PCR chip material in the simulation, and the most efficient material was evaluated using relative deviation and average square of difference. After assessing which material is the best choice, the diameter and length of the design were changed to determine the effect of varying the cross-sectional area of the fluid path to the fluid temperature. The first design has a diameter of 300μm, length of 200μm, and cross-sectional area of 130686 μm^2. Meanwhile, the second design has a diameter of 500μm, length of 300μm, and cross-sectional area of 346350 μm^2.

3. Results and Discussion

Designing and analyzing microfluidic PCR chips require a wide range of capabilities, which ANSYS 14.5 CFD provides. This enables engineers to evaluate various design factors and maximize chip performance by simulating complex fluid movement, heat transfer, and chemical reactions inside the device [27]. The software is appropriate for modelling biological reactions and fluid dynamics in microscale environments since it has advanced capacities like multiphase flow modeling, species transport, and surface reactions [28]. Engineers may look at and improve on important elements including channel shape, valve actuation, mixing effectiveness, and temperature management by using ANSYS 14.5 CFD. They may check potential design problems and enhance chip performance prior to production owing to the precise information on fluid velocity profiles, pressure distributions, residence duration, and temperature gradients of the software [29,30]. Issues that could occur while operating a chip can be found and mitigated using ANSYS 14.5 CFD.

 doi:10.20944/preprints202305.1033.v2

Regarding the potential for air bubbles, sedimentation, uneven heating, and uneven flow distribution, which can all have a detrimental impact on PCR performance and yield incorrect data, is part of this. The improved chip designs produced using ANSYS 14.5 CFD simulations result in higher sensitivity, decreased reaction time, and improved amplification efficiency, which eventually improve the accuracy and reliability of molecular biology investigations carried out on microfluidic PCR chips [31].

Using the data listed in Table 3, three designs were modeled with one having no loops, one having only a loop, and one having two loops. The copper plate for all three was set at a temperature of 58°C, and the designs were simulated using ANSYS 14.5 CFD. As shown in Table 4, as the number of loops is increased, the relative deviation also increases which indicates that the efficiency of the design decreases; however, the decrease is not that significant. The simulation shows that a fluid temperature maintained within 58°C, the relative deviation for the design with no loops is 0.65, with one loop is 0.80, and with two loops is 0.88. This decreasing trend is indicative of decreasing efficiency but only to a minimal extent. Therefore, looping can be used in designing the microfluidic PCR chip to reduce the chip length and to increase the residence time of the sample inside the device.

Table 4. The effect of looping on the efficiency of the design based on the calculation of relative deviation and ASD.

Design	Relative Deviation	ASD[a]
No Loop	0.65	1.12
One Loop	0.80	1.39
Two Loops	0.88	1.52

[a] $Average\ square\ of\ difference\ (\Delta T^2/n)$.

The efficiency of reactant mixing is improved by looping in the design of microfluidic PCR chips, which boosts amplification performance [32,33]. Looping enables the controlled transport and dispersion of target DNA, primers, and enzymes by providing circular flow channels within the chip. The looping structures induce vortices and turbulence that speed up the reaction rate by promoting reactant collision and contact [34]. Additionally, looping lessens the effects of diffusion and permits complete mixing of the reactants even in small volumes. This enhances the reaction's homogeneity and lessens the possibility of non-specific amplification. In order to improve mixing efficiency within the microfluidic PCR chip, looping design solutions, such as serpentine channels or spiral topologies, efficiently harness the advantages of fluidic looping [35,36].

For the simulation of the proposed microfluidic PCR chip, the designs drawn using ANSYS 14.5 CFD are shown in Figure 3. The five copper plates seen in Figure 3(b) were set at temperatures 58°C, 72°C, 95°C, 72°C, and 58°C for the first simulation, temperatures 60°C, 74°C, 97°C, 74°C, and 60°C for the second simulation, and temperatures 63°C, 77°C, 100°C, 77°C, and 63°C for the third simulation for each material (the order of temperatures corresponds to the order of plates seen in the figure).

Preprints (www.preprints.org) | NOT PEER-REVIEWED | Posted: 10 August 2023 doi:10.20944/preprints202305.1033.v2

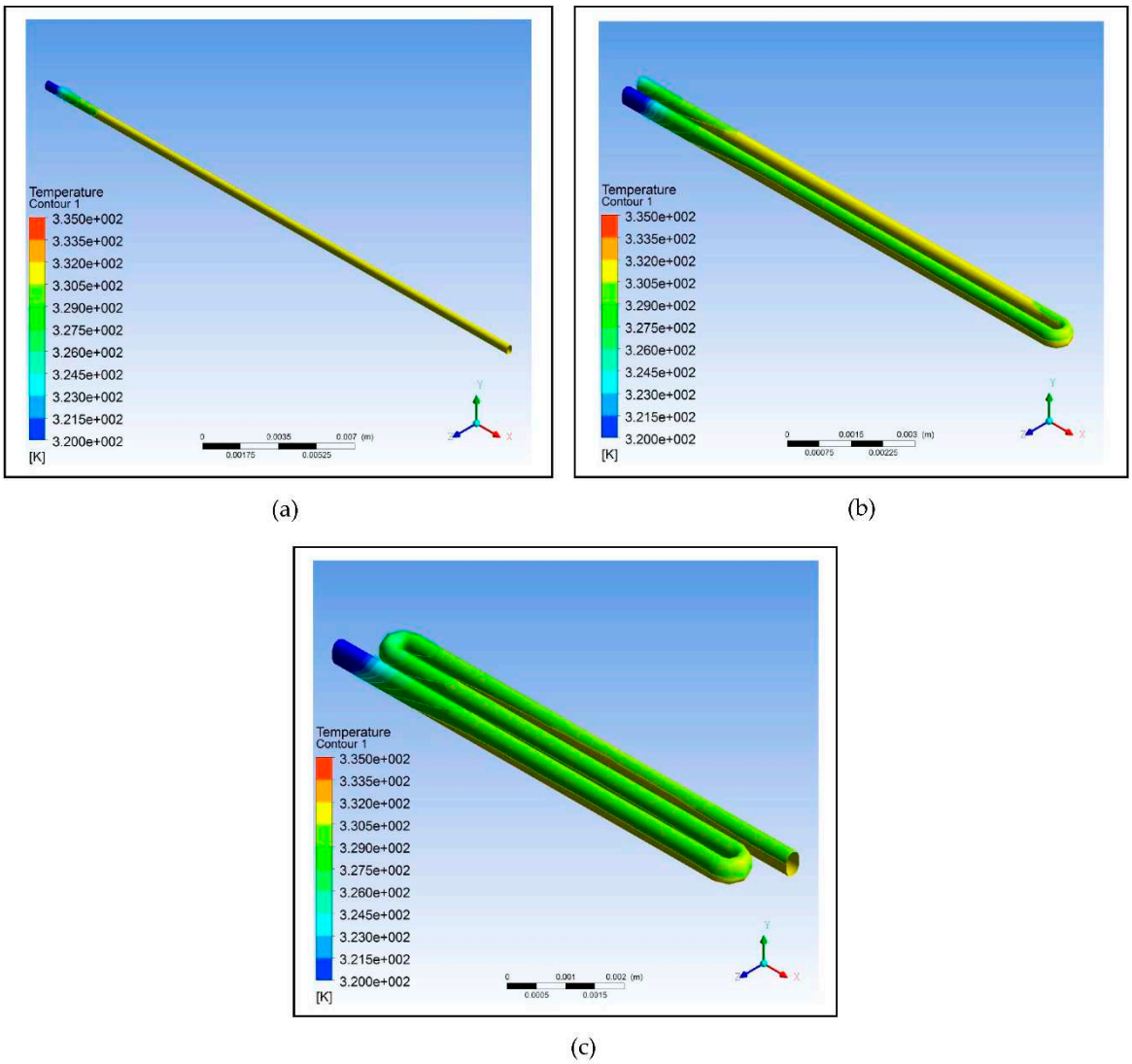

Figure 2. Using ANSYS 14.5 Computational Fluid Dynamics (CFD), the designs intended to test the effect of looping on the efficiency of the device were modelled: (**a**) Design with no loops; (**b**) Design with one loop; (**c**) Design with two loops.

Thermal cycling, which involves heating and cooling the reaction mixture at particular temperatures for DNA amplification, is an essential procedure in microfluidic PCR chips. Thermal cycle efficiency can be greatly improved by using looping design concepts. The chip design can enhance the surface area accessible for heat transfer by including loops and complicated routes [37]. As a result, the fluid and the chip material surrounding it may exchange heat more effectively, improving the temperature homogeneity of the reaction mixture [38]. For reliable and constant amplification results, efficient heat dissipation and minimal temperature changes are made possible by the looping structures. The vast range of simulation tools provided by ANSYS 14.5 CFD are essential for creating microfluidic PCR chips with the best possible thermal cycling [39]. The software enables engineers to evaluate and optimize numerous design parameters by simulating heat transfer, fluid flow, and temperature distribution within the chip. Engineers can examine the effects of chip geometry, channel dimensions, and materials on temperature distribution during thermal cycling with ANSYS 14.5 CFD simulations [40]. The software helps identify potential hotspots or temperature changes that could impact the PCR process by providing insights into variables including convective heat transfer, conductive heat dissipation, and radiative heat exchange [41]. By offering a virtual environment to investigate and improve different thermal cycle factors, ANSYS 14.5 CFD considerably cuts down on the time and expense of experimental trial and error [42]. Because it can mimic various temperature profiles, cycling rates, and thermal profiles, chip designs may be

Preprints (www.preprints.org) | NOT PEER-REVIEWED | Posted: 10 August 2023 doi:10.20944/preprints202305.1033.v2

evaluated and optimized quickly. Additionally, it provides in-depth representations of temperature distributions, enabling users to see potential temperature changes or places with inadequate temperature control [43]. To maintain uniform temperature distribution and reduce temperature swings during thermal cycling, designers can optimize chip shape, channel layout, and thermal management strategies by understanding the heat transfer processes within the chip [44]. The evaluation of chip performance under various operating conditions is made easier with ANSYS 14.5 CFD. To assess the durability and reliability of the microfluidic PCR chip design, it can simulate changes in sample volume, flow rates, and ambient temperature [45]. The detection of possible problems and the tuning of thermal cycle parameters for improved performance are made easier with the use of this information.

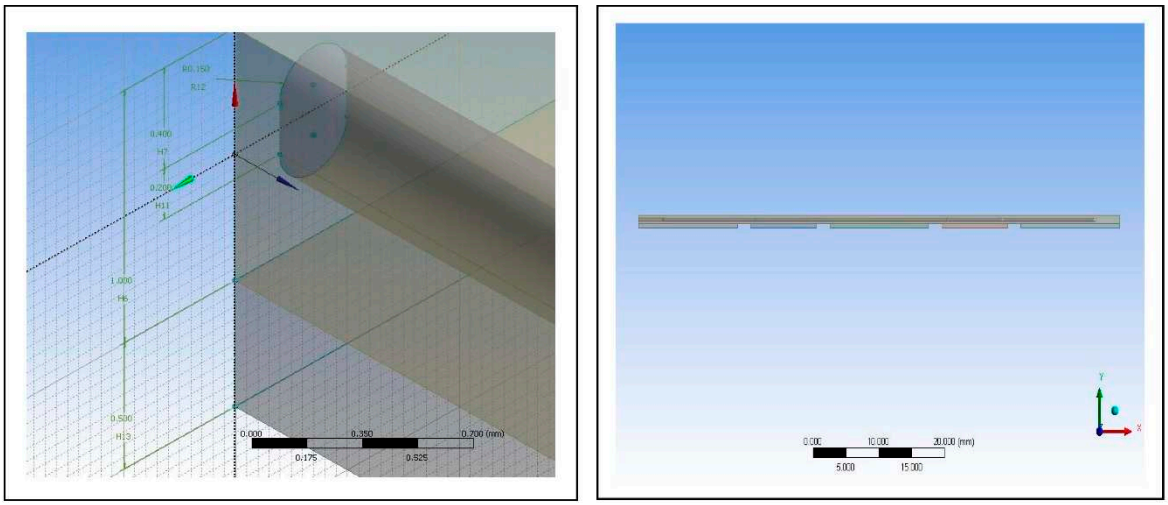

(a) (b)

Figure 3. Images of the proposed microfluidic PCR chip design modelled from ANSYS 14.5 Computational Fluid Dynamics (CFD): (**a**) Microfluidic chip dimensions; (**b**) Microfluidic chip side view.

The final design is illustrated in Figure 4, showing a 44-cycle microfluidic PCR chip design.

In microfluidic PCR chips, the cycle number is crucial for maximizing amplification effectiveness. The possibility of DNA amplification is increased by increasing the number of cycles, especially for low-copy targets [46]. The concentration of the target DNA molecules rises exponentially as the number of cycles is increased, enhancing sensitivity and detection limits [47]. However, to prevent non-specific amplification, which might produce false-positive results, the cycle number must be properly noted of. When unwanted DNA fragments are amplified together with the target DNA, this is known as non-specific amplification [48]. By making sure that the target sequence is specifically amplified for, optimizing the cycle number improves the accuracy of the PCR chip. Furthermore, the entire reaction time needed for DNA amplification in microfluidic PCR chips is directly influenced by the number of cycles [49]. The overall reaction time increases as the cycle number rises, which might be an important factor for applications that require lower reaction time. By maximizing thermal cycling efficiency, decreasing heat transfer delays, and increasing temperature uniformity, microfluidic PCR chip designs should seek to speed up reaction times [50]. With the use of the computational fluid dynamics program ANSYS 14.5 CFD, thermal cycling in microfluidic PCR chips may be simulated and optimized, allowing to choose the right cycle number that will produce the required amplification in the least amount of time [51]. The power usage, as well as the heating and cooling requirements of the PCR chip, are influenced by the cycle number. Higher cycle numbers could necessitate more energy and stricter temperature control, which might have an impact on chip design factors including power supply, thermal management, and overall system complexity. It is crucial to carefully consider the desired DNA concentration, amplification sensitivity, time restrictions, and other performance requirements when determining the ideal cycle

Preprints (www.preprints.org) | NOT PEER-REVIEWED | Posted: 10 August 2023 doi:10.20944/preprints202305.1033.v2

number for a given application [52,53]. A balance between amplification efficiency, specificity, reaction time, and chip performance can be achieved by taking these parameters into account.

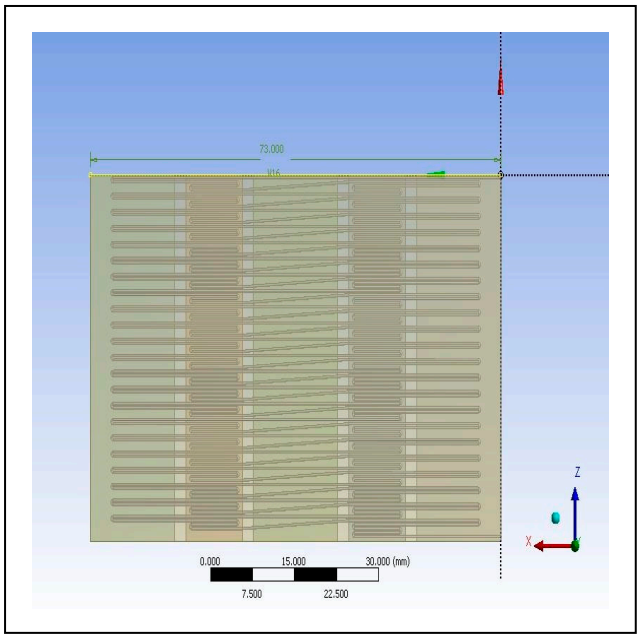

Figure 4. Image of the 44-cycle microfluidic PCR chip design modelled from ANSYS 14.5 Computational Fluid Dynamics (CFD).

However, during the meshing procedure on the ANSYS 14.5 CFD, the software cannot mesh the design due to its limitation since the program is only accessible for educational use. Instead of meshing the whole design, only a 2-cycle microfluidic PCR chip design was meshed and simulated as representative of the 44-cycle microfluidic PCR chip design.

Furthermore, different polymeric materials were tested to determine which is the best choice to be used for designing the microfluidic chip. Figure 5 illustrates the simulation of the microfluidic PCR chip designs modelled from polypropylene set at various copper temperatures. Figure 6 illustrates the simulation of the microfluidic PCR chip designs modelled from polycarbonate set at various copper temperatures. And Figure 7 illustrates the simulation of the microfluidic PCR chip designs modelled from polydimethylsiloxane set at various copper temperatures.

Polypropylene demonstrates a number of significant benefits that make it suitable for microfluidic PCR chip design. Polypropylene is chemically inert, which makes it extremely resistant to a variety of chemicals and solvents used in PCR operations [54]. This characteristic guarantees that polypropylene does not affect the amplification reaction, resulting in precise and trustworthy results. Polypropylene is also biocompatible, which reduces the chance of sample contamination and offers an ideal setting for PCR reactions. Comparing polypropylene to other materials like glass or silicon, it is more affordable. Microfluidic PCR chips may be produced in large quantities owing to its affordable manufacturing costs, increasing their availability to researchers and healthcare workers [55]. Additionally, polypropylene is simple to shape, making it possible to create intricate patterns with exact geometries and microfluidic elements. Furthermore, a crucial factor for PCR applications is heat stability. Repeated heating and cooling cycles are necessary for microfluidic PCR chips to achieve DNA denaturation, annealing, and extension. With a melting point of roughly 160–170°C and a glass transition temperature of roughly –10°C, polypropylene has good thermal stability [56]. With the aid of these characteristics, the microfluidic PCR chip is able to resist the temperature cycling necessary for PCR without deforming or losing structural integrity. Due to the poor thermal conductivity of polypropylene, there is less heat transmission between the various areas of the microfluidic chip, which allows for effective temperature control and less sample contamination [57].

 doi:10.20944/preprints202305.1033.v2

By maintaining well defined heat zones for each reaction step, this characteristic guarantees that the PCR process is accurate and specific.

Real-time observation and analysis of PCR reactions are made possible by the optical transparency of polycarbonate. This characteristic makes it possible for researchers to monitor and measure the amplification procedure, leading to precise and accurate results. Polycarbonate has exceptional chemical resistance, making it work with a variety of PCR reagents and lowering the possibility of sample contamination [58]. The microfluidic PCR chip is long-lasting due to its resistance to chemical deterioration, making it a good material for recurrent use. Also, polycarbonate is non-toxic and biocompatible, limiting disruption of biological material and maintaining the integrity of DNA amplification [59]. These qualities also make polycarbonate a suitable material for microfluidic PCR chip applications since they are essential for preserving the precision and dependability of PCR results. Because polycarbonate has a low thermal conductivity, there is less heat transfer between the various parts of the microfluidic chip. This characteristic makes it easier to effectively control the temperature within designated reaction zones, reducing the risk of cross-contamination and preserving the precision and specificity of the PCR procedure [60]. The temperature cycling of the microfluidic PCR chip is more consistent due to the low coefficient of thermal expansion of polycarbonate. Enhancing the reliability of PCR results and minimizing fluctuations in DNA amplification efficiency are temperature profiles that are constant across the chip. The microfluidic PCR chip design can also benefit from hydrophobic properties of the polymer [61]. It does not require further surface alterations or coatings because of its inherent hydrophobicity, which enables precise control of fluid flow. This characteristic lowers the possibility of sample evaporation during the PCR process and improves the compatibility of polycarbonate microfluidic PCR chips with PCR chemicals [62].

Due to its great flexibility and elastomeric properties, polydimethylsiloxane (PDMS) makes it simple to fabricate intricate microfluidic devices. It is simple to mold or pattern to make complex features and structures, which makes it easier to incorporate several functionalities into a single chip [63,64]. The adaptability and use of microfluidic PCR chips are increased by the flexibility of PDMS, which also makes it possible to connect tubing and other components in a simple manner. In comparison to other materials like glass or silicon, PDMS is also a more affordable choice. Microfluidic PCR chips can be produced in large quantities thanks to its affordable manufacturing costs, which increases their accessibility for researchers and medical experts [65]. Precision temperature control within designated reaction zones is made possible by the poor thermal conductivity of PDMS, which reduces heat transmission between various areas of the microfluidic chip. This characteristic improves the precision and specificity of the PCR process and lowers the possibility of sample contamination. Due to its low coefficient of thermal expansion, PDMS also provides good thermal cycling performance [66]. With this feature, the microfluidic PCR chip is guaranteed to have constant temperature profiles, which minimizes changes in DNA amplification efficiency and enhances the repeatability of results. Additionally, PDMS demonstrates hydrophobic characteristics that can be used to regulate fluid flow inside the microfluidic device [67]. The hydrophobic properties of PDMS make it easier for well-defined channels and droplets to develop, providing fine-grained control over the transport of samples and reagents [68]. This characteristic lowers the possibility of sample evaporation during the PCR process and improves the compatibility of PDMS microfluidic PCR chips with various PCR reagents.

Preprints (www.preprints.org) | NOT PEER-REVIEWED | Posted: 10 August 2023 doi:10.20944/preprints202305.1033.v2

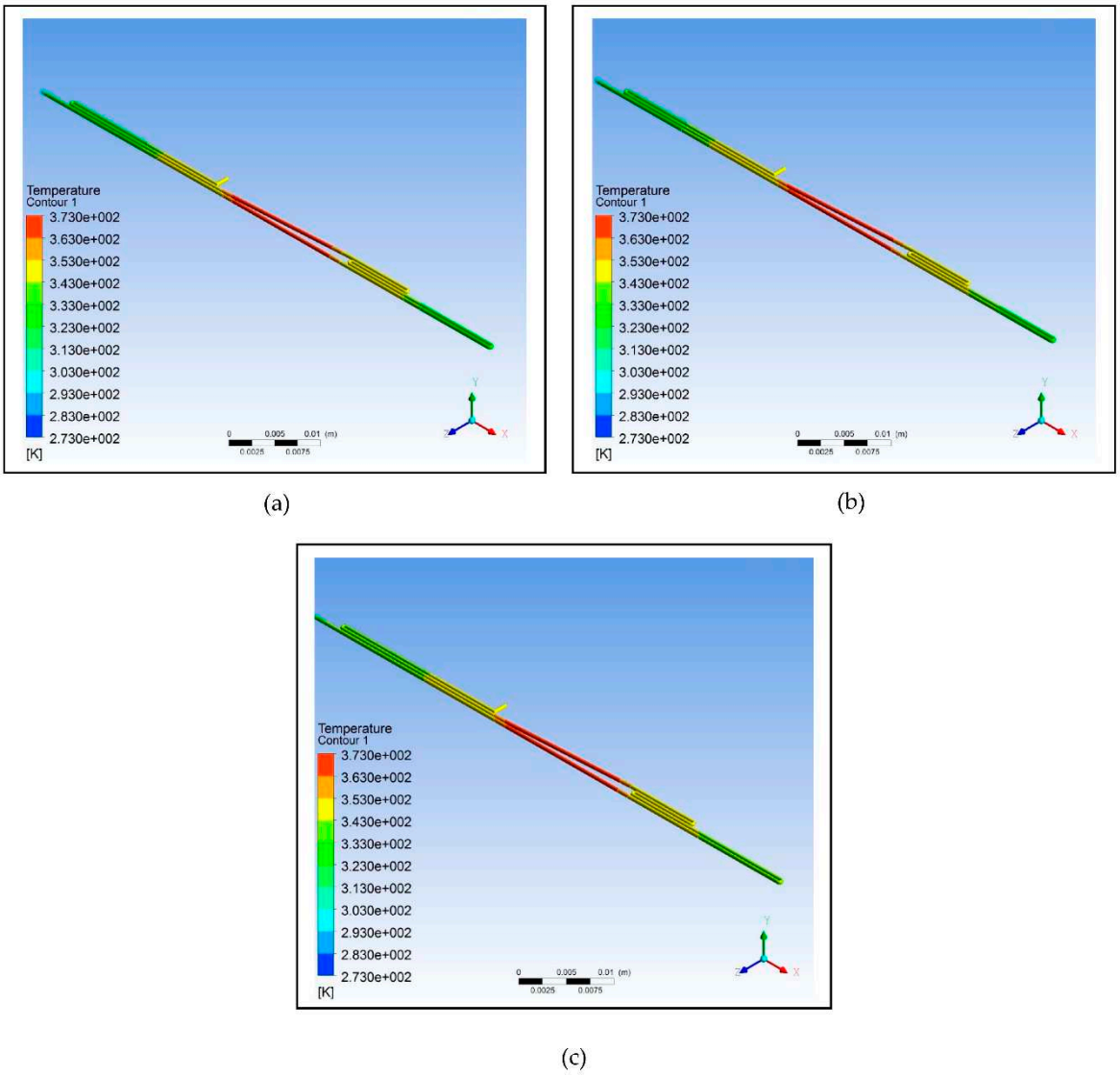

Figure 5. Polypropylene microfluidic PCR chip design set at temperatures of: (**a**) 58°C (annealing), 72°C (extension), and 95°C (denaturation); (**b**) 60°C (annealing), 74°C (extension), and 97°C (denaturation); (**c**) 63°C (annealing), 77°C (extension), and 100°C (denaturation).

Preprints (www.preprints.org) | NOT PEER-REVIEWED | Posted: 10 August 2023 doi:10.20944/preprints202305.1033.v2

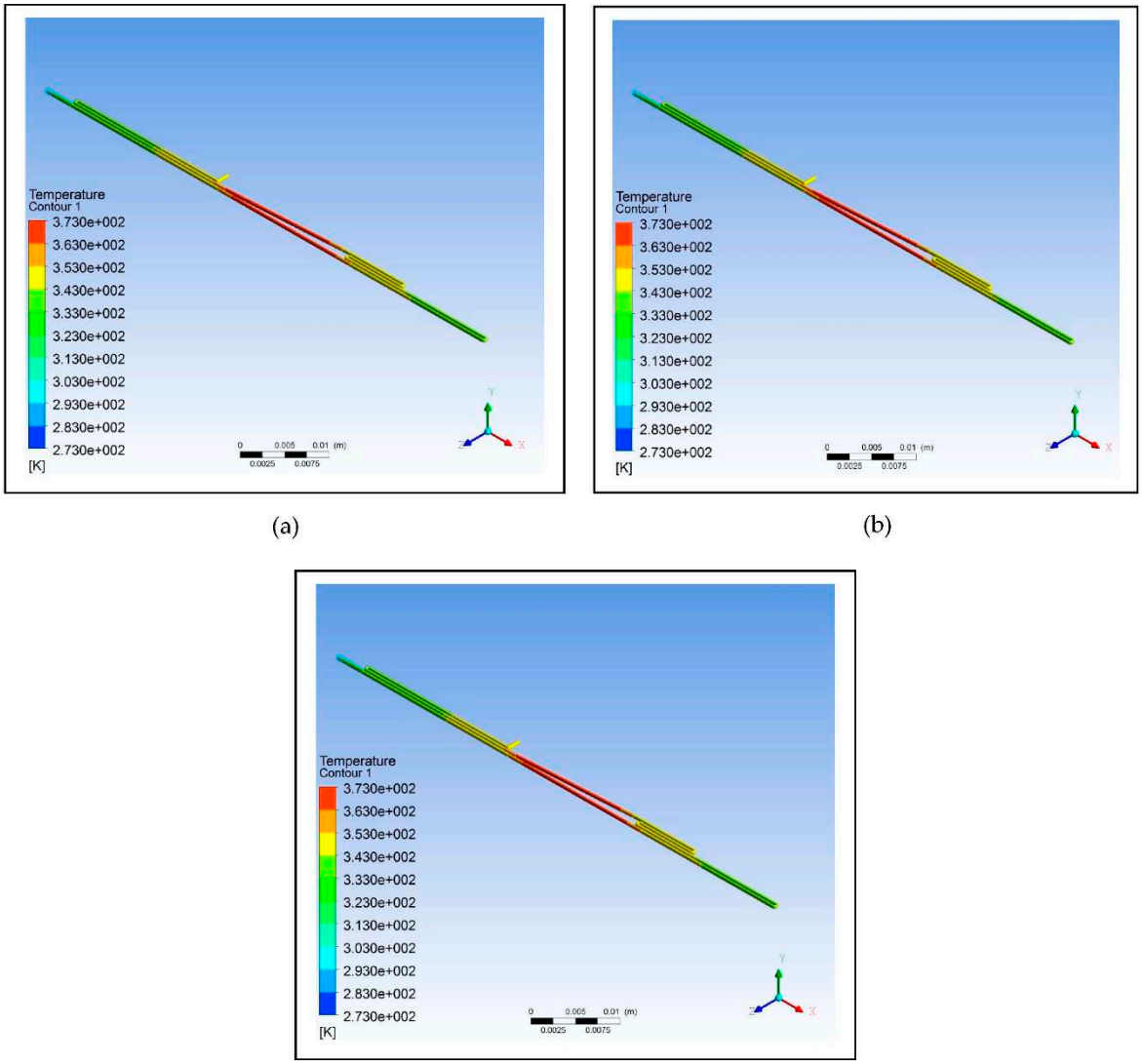

Figure 6. Polycarbonate microfluidic PCR chip design set at temperatures of: (**a**) 58°C (annealing), 72°C (extension), and 95°C (denaturation); (**b**) 60°C (annealing), 74°C (extension), and 97°C (denaturation); (**c**) 63°C (annealing), 77°C (extension), and 100°C (denaturation).

Preprints (www.preprints.org) | NOT PEER-REVIEWED | Posted: 10 August 2023 doi:10.20944/preprints202305.1033.v2

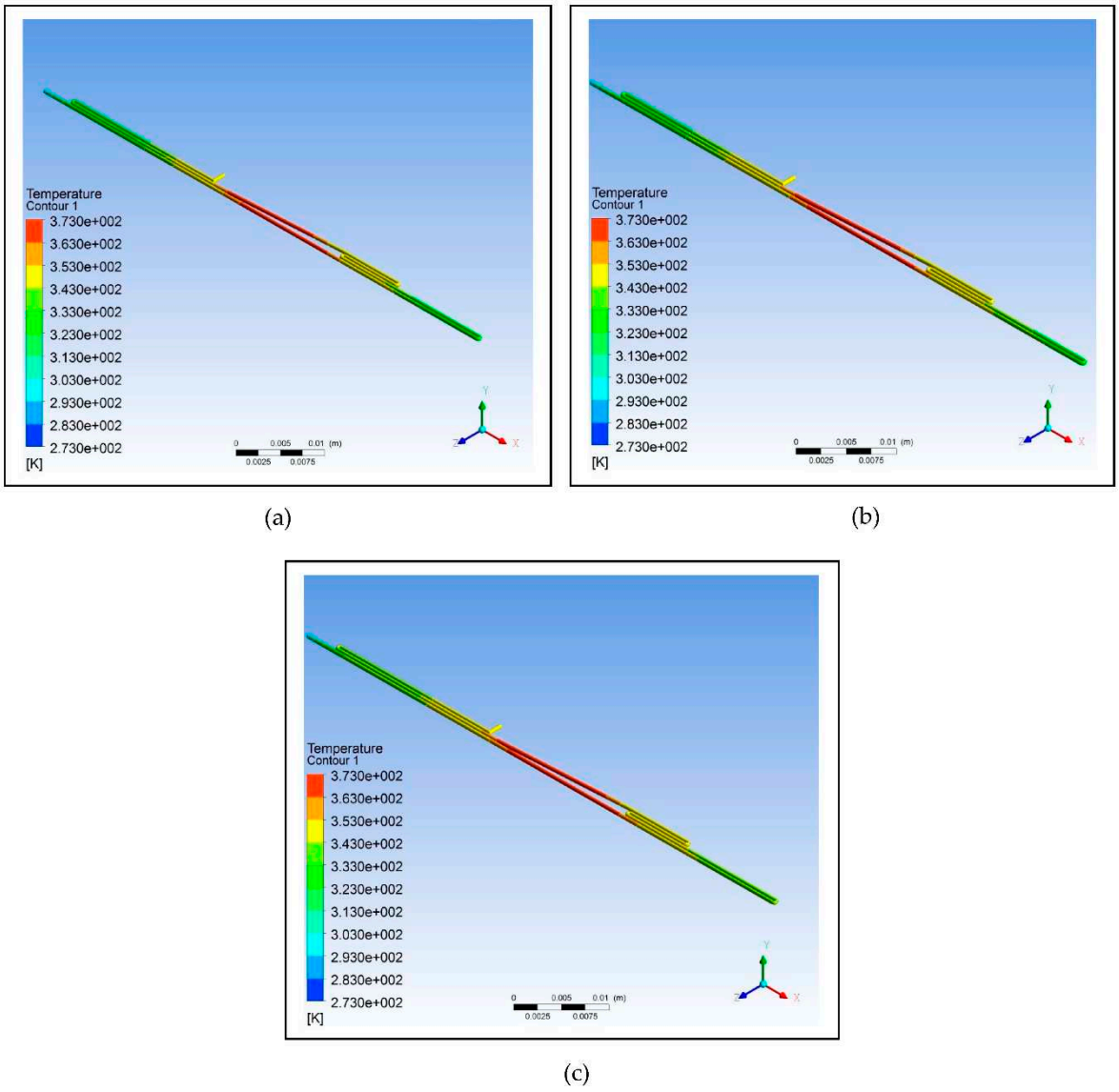

Figure 7. Polydimethylsiloxane microfluidic PCR chip design set at temperatures of: (**a**) 58°C (annealing), 72°C (extension), and 95°C (denaturation); (**b**) 60°C (annealing), 74°C (extension), and 97°C (denaturation); (**c**) 63°C (annealing), 77°C (extension), and 100°C (denaturation).

Using the data at different nodes generated from the various simulations, the relative deviation and average square of difference (ASD) were calculated as shown in Table 5.

Table 5. The effect of the different polymeric materials under various temperatures on the efficiency of the design based on the calculation of relative deviation and ASD.

	58°C, 72°C, 95°C		60°C, 74°C, 97°C		63°C, 77°C, 100°C	
Material	**Relative Deviation**	**ASD[d]**	**Relative Deviation**	**ASD[d]**	**Relative Deviation**	**ASD[d]**
PP[a]	0.94	3.21	2.84	5.82	6.90	25.00
PC[b]	1.92	8.61	3.15	10.00	6.92	26.70
PDMS[c]	2.78	14.00	3.47	14.00	6.93	29.00

[a] *Polypropylene*
[b] *Polycarbonate*
[a] *Polydimethysiloxane*
[d] *Average square of difference* ($\Delta T^2/n$).

Preprints (www.preprints.org) | NOT PEER-REVIEWED | Posted: 10 August 2023 doi:10.20944/preprints202305.1033.v2

The results show that polypropylene set at a copper plate temperature of 58°C for annealing, 72°C for extension, and 95°C for denaturation has the lowest relative deviation of 0.94 and lowest average square of difference ($\Delta T^2/n$) of 3.21. This suggests that polypropylene under this set condition is the most efficient material to use in fabricating the microfluidic PCR chip.

Relative deviation was intended to measure the precision or the consistency of results that can be generated from the designed microfluidic PCR chip. It measures the variance between subsequent readings of the same measurement or replication of the DNA amplification procedure [69]. An extremely high degree of precision and reproducibility is implied by a low relative deviation, which shows little variation in the amplification results. Achieving a minimal relative variation in the design of microfluidic PCR chips is essential for precise and dependable DNA amplification. It indicates that there is less chance of false-positive or false-negative results because of the ability of the PCR chip to enable consistent and repeatable results [70]. In applications like diagnostics or research trials, where consistency and reproducibility are crucial, a low relative deviation assures that the chip generates accurate data. Conversely, the average square of difference was intended to measure the accuracy or efficiency of the proposed design. It measures the difference between the actual outcomes of the amplification and the desired or anticipated values. The chip design produces accurate amplification results with little departure from the expected values, as indicated by a low average square of difference. In order to achieve precise DNA amplification while designing microfluidic PCR chips, a low average square of difference must be attained [71]. A low value denotes effective reaction parameter control by the chip design, including control of temperature, reagent concentrations, and fluid flow, leading to accurate and dependable amplification [72]. The likelihood of experimental mistakes, erroneous results, or the necessity for additional testing is reduced by a precise chip design.

Consequently, after figuring out that polypropylene is the best option, the microfluidic PCR chip with this design set under the optimum temperatures of 58°C, 72°C, and 95°C was subjected to further testing by changing the parameters, while unchanging the inlet velocity of the models. Figure 8 illustrates the results of the simulations, and Table 6 shows the relative deviation and average square of difference (ASD) calculated from the two designs.

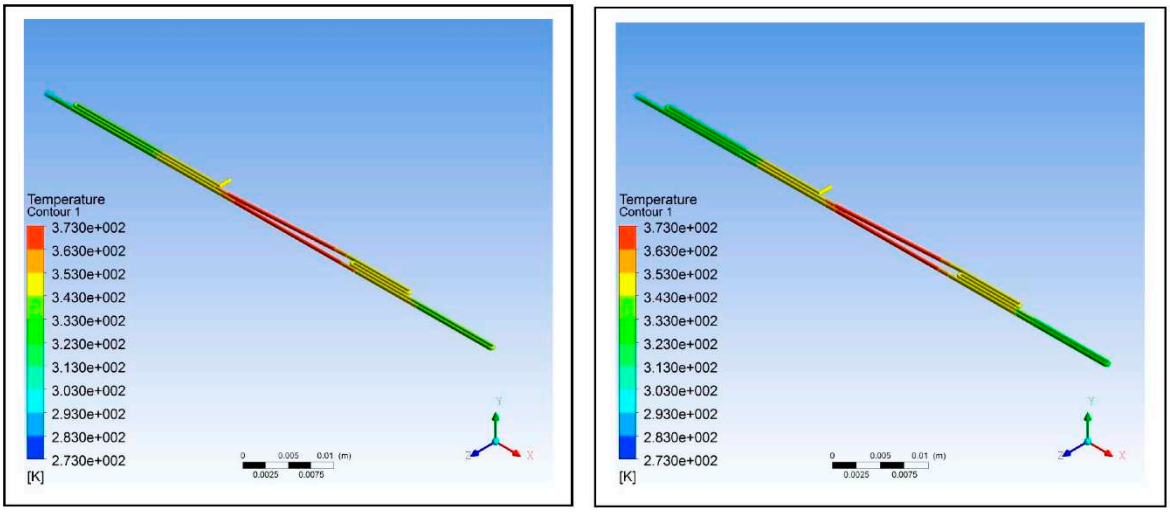

(a) (b)

Figure 8. Polypropylene microfluidic PCR chip design set at temperatures of 58°C (annealing), 72°C (extension), and 95°C (denaturation) with dimensions of: (**a**) 300 μm (diamater), 200 μm (length), and 130686 μm² (cross-sectional area); (**b**) 500 μm (diamater), 300 μm (length), and 346350 μm² (cross-sectional area).

 doi:10.20944/preprints202305.1033.v2

Table 6. The effect of changing the parameters of the polypropylene microfluidic PCR chip under the temperatures of 58°C (annealing), 72°C (extension), and 95°C (denaturation) on the efficiency of the design based on the calculation of relative deviation and ASD.

Parameter	Design 1	Design 2
Diameter	300	500
Length	200	300
Relative Deviation	0.94	2.31
ASD[a]	3.21	5.96

[a] $Average\ square\ of\ difference\ (\Delta T^2/n)$.

The data shows that increasing the diameter and length of the fluid path affects the fluid temperature. Increasing the cross-sectional area using the same inlet velocity of the fluid flowing through the chip also results in the increase of relative deviation and ASD indicating a decrease in efficiency of reaching the set temperature at different zones. Thus, the design using a smaller cross-sectional area is most suitable to use because of its comparatively lower relative deviation and ASD, which predispose it to be favored more in fabricating the device.

Since one of the aims of this study is to reduce the cost of the device for public access, limiting material utilization was necessary in order to compensate for this. Miniaturizing the conventional PCR through fabricating a more portable and relatively smaller device would surely affect its efficiency in detecting Malaria, especially in the amplification process [73]. The proposed microfluidic PCR chip is designed to detect malaria even with a small sample volume while, at the same time, not compromising the specificity of the test. The threshold cycle of the conventional PCR amplification of *P.falciparum* DNA fragments is 36 with a threshold sensitivity of 0.2 parasite per 1 μL [74]. However, the proposed microfluidic PCR chip was designed for 44 cycles because it is also intended to detect small samples, which need to be amplified more compared to samples of greater volume. The amount of time it takes for the microfluidic PCR chip to amplify the sample for a given number cycles was evaluated (see S3). In 44 cycles, which the device was specifically designed for, consumes around 112.23 minutes to complete the process.

4. Conclusion

The simulation shows that looping can affect the temperature of the fluid to a minimal extent, and therefore, can be considered in designing a microfluidic PCR chip in order to decrease the chip length. Based on the simulation, the best material for designing the microfluidic PCR chip is polypropylene with a relative deviation of 0.94 from the set temperatures of 58°C (annealing), 72°C (extension), and 95°C (denaturation). It was also proven that increasing the cross-sectional area of the fluid path can have an effect on the temperature of the fluid; thus, it is recommended to use a smaller cross-sectional area to ensure that the set temperatures in different zones are reached. With the objectives this simulative study aims to answer, the results generated from this intend to serve as a preliminary screening towards an optimized design of a microfluidic-based PCR device for *P. falciparum* DNA fragment amplification.

As mentioned earlier, only a 2-cycle microfluidic chip design was meshed due to the limitation of the software. Future researchers might want to take a look at this and try to mesh the 44-cycle microfluidic chip used in this study. Other parameters may be tested as well for their effect on the efficiency of the device in detecting malaria, and other materials may be assessed to broaden the application of this design.

Supplementary Materials: The following supporting information can be downloaded at the website of this paper posted on Preprints.org. Figure S1: title; Table S1: title; Video S1: title.

References

1. N. Sakihama, T. Mitamura, A. Kaneko, T. Horii, K. Tanabe, Long PCR Amplification of Plasmodium falciparum DNA Extracted from Filter Paper Blots, Exp Parasitol. 97 (2001) 50–54. https://doi.org/10.1006/EXPR.2000.4591.
2. F. Ansah, J. Suurbaar, D. Darko, N.G. Anabire, S.O. Blankson, B.K.S. Domson, A. Soulama, P. Kpasra, J.D. Chirawurah, L. Amenga-Etego, P. Kanyong, G.A. Awandare, Y. Aniweh, Development of Cooperative Primer-Based Real-Time PCR Assays for the Detection of Plasmodium malariae and Plasmodium ovale, The Journal of Molecular Diagnostics. 23 (2021) 1393–1403. https://doi.org/10.1016/J.JMOLDX.2021.07.022.
3. W.A. Azmi, A.F.M. Rizki, Y. Djuardi, I.M. Artika, J.E. Siregar, Molecular insights into artemisinin resistance in Plasmodium falciparum: An updated review, Infection, Genetics and Evolution. 112 (2023) 105460. https://doi.org/10.1016/J.MEEGID.2023.105460.
4. H. Torkashvand, S.A. Dehdast, M. Nateghpour, A.M. Haghi, G.C. Fard, T. Elmi, M. Shabani, F. Tabatabaie, Antimalarial nano-drug delivery system based on graphene quantum dot on Plasmodium falciparum: Preparation, characterization, toxicological evaluation, Diam Relat Mater. 132 (2023) 109670. https://doi.org/10.1016/J.DIAMOND.2022.109670.
5. G.C. Chemwor, B.M. Andagalu, I.A. Onyango, B.H. Opot, R.O. Okoth, R.A. Yedah, J.A. Juma, E.W. Mwakio, D.M. Wakoli, J.G. Amwoma, A.C. Cheruiyot, D.W. Juma, B.R. Ogutu, T.E. Egbo, E.C. Garges, A.L. Roth, E. Kamau, O.J. Watson, H.M. Akala, Therapeutic response to artemisinin combination therapies among individuals with Plasmodium falciparum single infection vs mixed Plasmodium species infections: a retrospective posthoc analysis in Kisumu County, western Kenya, International Journal of Infectious Diseases. 132 (2023) 17–25. https://doi.org/10.1016/J.IJID.2023.04.008.
6. S.-J. Xu, H.-M. Shen, Y.-B. Cui, S.-B. Chen, B. Xu, J.-H. Chen, Genetic diversity and natural selection of rif gene (PF3D7_1254800) in the Plasmodium falciparum global populations, Mol Biochem Parasitol. 254 (2023) 111558. https://doi.org/10.1016/J.MOLBIOPARA.2023.111558.
7. L. Dong, W. Li, Q. Xu, J. Gu, Z. Kang, J. Chen, X. Xu, X. Zhang, X. Zhang, H. Jiang, M. Guan, A rapid multiplex assay of human malaria parasites by digital PCR, Clinica Chimica Acta. 539 (2023) 70–78. https://doi.org/10.1016/J.CCA.2022.12.001.
8. A. Taghdiri, P.G. Nejad Almani, I. Sharifi, M.A. Mohammadi, S. Salari, Detection of malaria with light microscopy and Nested polymerase chain reaction (Nested PCR) methods in peripheral blood expansions and investigation of the genetic diversity of Plasmodium species by 18S rRNA gene in Southeast of Iran, Microb Pathog. 137 (2019) 103782. https://doi.org/10.1016/J.MICPATH.2019.103782.
9. C.R.F. Chagas, J. Harl, G. Valkiūnas, Co-infections of Plasmodium relictum lineages pSGS1 and pGRW04 are readily distinguishable by broadly used PCR-based protocols, with remarks on global distribution of these malaria parasites, Acta Trop. 217 (2021) 105860. https://doi.org/10.1016/J.ACTATROPICA.2021.105860.
10. H. Frickmann, C. Wegner, S. Ruben, C. Behrens, H. Kollenda, R. Hinz, S. Rojak, N.G. Schwarz, R.M. Hagen, E. Tannich, Evaluation of the multiplex real-time PCR assays RealStar malaria S&T PCR kit 1.0 and FTD malaria differentiation for the differentiation of Plasmodium species in clinical samples, Travel Med Infect Dis. 31 (2019) 101442. https://doi.org/10.1016/J.TMAID.2019.06.013.
11. H. Mirahmadi, M. Rahmati-Balaghaleh, M. Afzalaghaee, M. Zarean, S.A. Shamsian, A. Mehravaran, V. Raissi, S. Etemadi, Detection of malaria using blood smear by light microscopy, RDT and nested-PCR for suspected patients in south-eastern Iran, Gene Rep. 25 (2021) 101339. https://doi.org/10.1016/J.GENREP.2021.101339.
12. X. Xiong, A. Hou, S. Yi, Y. Guo, Z. Zhao, Z. Wu, H. Cheng, K. Li, Z. Li, Y. Ren, Y. Wang, Analysis of oral microorganism diversity in healthy individuals before and after chewing areca nuts using PCR-denatured gradient gel electrophoresis, Animal Nutrition. 4 (2018) 294–299. https://doi.org/10.1016/J.ANINU.2018.07.001.
13. A. El-Latif Hesham, V.K. Gupta, B.P. Singh, Use of PCR-denaturing gradient gel electrophoresis for the discrimination of Candida species isolated from natural habitats, Microb Pathog. 120 (2018) 19–22. https://doi.org/10.1016/J.MICPATH.2018.04.027.
14. C. Banerjee, S. Nag, M. Goyal, D. Saha, A.A. Siddiqui, S. Mazumder, S. Debsharma, S. Pramanik, U. Bandyopadhyay, Nuclease activity of Plasmodium falciparum Alba family protein PfAlba3, Cell Rep. 42 (2023) 112292. https://doi.org/10.1016/J.CELREP.2023.112292.
15. S.-J. Xu, H.-M. Shen, Y.-B. Cui, S.-B. Chen, B. Xu, J.-H. Chen, Genetic diversity and natural selection of rif gene (PF3D7_1254800) in the Plasmodium falciparum global populations, Mol Biochem Parasitol. 254 (2023) 111558. https://doi.org/10.1016/J.MOLBIOPARA.2023.111558.
16. Y. Wu, S. Leyk, H. Torabi, K. Höhn, B. Honecker, M. del P.M. Tauler, D. Cadar, T. Jacobs, I. Bruchhaus, N.G. Metwally, Plasmodium falciparum infection reshapes the human microRNA profiles of red blood cells and their extracellular vesicles, IScience. 26 (2023) 107119. https://doi.org/10.1016/J.ISCI.2023.107119.

17. Z. Xiang, D. Li, S. Wang, T. Shen, W. He, M. Li, W. Zeng, X. Chen, Y. Wu, L. Cui, Z. Yang, A simple alkali lysis method for Plasmodium falciparum DNA extraction from filter paper blood samples, Mol Biochem Parasitol. 254 (2023) 111557. https://doi.org/10.1016/J.MOLBIOPARA.2023.111557.
18. D. Choubey, B. Deshmukh, A.G. Rao, A. Kanyal, A.K. Hati, S. Roy, K. Karmodiya, Genomic analysis of Indian isolates of Plasmodium falciparum: Implications for drug resistance and virulence factors, Int J Parasitol Drugs Drug Resist. 22 (2023) 52–60. https://doi.org/10.1016/J.IJPDDR.2023.05.003.
19. A. Ebrahimzadeh, B. Fouladi, A. Fazaeli, High rate of detection of mixed infections of Plasmodium vivax and Plasmodium falciparum in South-East of Iran, using nested PCR, Parasitol Int. 56 (2007) 61–64. https://doi.org/10.1016/J.PARINT.2006.12.001.
20. A. Wångdahl, R.T. Bogale, I. Eliasson, I. Broumou, F. Faroogh, F. Lind, G. Vashchuk, A. Hildell, S. Franson, E. Hallberg, I. Grip, I. Nordling, A. Gervin, S. Kaitoly, B. Tekleab, K. Wyss, A. Requena-Méndez, O. Hertting, A. Färnert, Malaria parasite prevalence in Sub-Saharan African migrants screened in Sweden: a cross-sectional study, The Lancet Regional Health - Europe. 27 (2023) 100581. https://doi.org/10.1016/J.LANEPE.2022.100581.
21. A.K.D.J. Fall, C. Dechavanne, A. Sabbagh, A. Garcia, D. Courtin, F. Migot-Nabias, Combined polymorphisms involving the IgG heavy chain and Fc gamma receptors among Fulani and non-Fulani in Benin: implications for the natural protection of young Fulani against Plasmodium falciparum malaria infections, Infection, Genetics and Evolution. 112 (2023) 105461. https://doi.org/10.1016/J.MEEGID.2023.105461.
22. C.C. Hermsen, D.S.C. Telgt, E.H.P. Linders, L.A.T.F. Van De Locht, W.M.C. Eling, E.J.B.M. Mensink, R.W. Sauerwein, Detection of Plasmodium falciparum malaria parasites in vivo by real-time quantitative PCR, Mol Biochem Parasitol. 118 (2001) 247–251. https://doi.org/10.1016/S0166-6851(01)00379-6.
23. N.E.P. Fernandas, H. Silveira, A.S. Franco, A.P. Arez, J.M. Forte, V.E. Do Rosário, Detection of malaria parasites in paraffin-embedded spleen and placental tissues by nested PCR, Trans R Soc Trop Med Hyg. 95 (2001) 293–294. https://doi.org/10.1016/S0035-9203(01)90237-8.
24. C. Maier, T. Calafut, Polypropylene: The Definitive User's Guide and Databook, Elsevier Science, 2008. https://books.google.dk/books?id=AWaSJd9Non8C.
25. H.E. Bair, D.R. Falcone, M.Y. Hellman, G.E. Johnson, P.G. Kelleher, Hydrolysis of polycarbonate to yield BPA, J Appl Polym Sci. 26 (1981) 1777–1786. https://doi.org/10.1002/APP.1981.070260603.
26. B.K. Gale, M.A. Eddings, S.O. Sundberg, A. Hatch, J. Kim, T. Ho, S.M. Karazi, Low-Cost MEMS Technologies, Reference Module in Materials Science and Materials Engineering. (2016). https://doi.org/10.1016/B978-0-12-803581-8.00530-0.
27. A.P. Agrawal, S. Ali, S. Rathore, Finite element stress analysis for shape optimization of spur gear using ANSYS, Mater Today Proc. 64 (2022) 1147–1152. https://doi.org/10.1016/J.MATPR.2022.03.404.
28. M. Karthick, C. Siva Ramakrishna, R. Pugazhenthi, N. Gudadhe, S. Baskar, Renu, R. Kumar, Contact stress analysis of xylon coated spur gear using ANSYS workbench, Mater Today Proc. (2023). https://doi.org/10.1016/J.MATPR.2023.03.572.
29. A. Chinnamahammad Bhasha, K. Balamurugan, Fracture analysis of fuselage wing joint developed by aerodynamic structural materials, Mater Today Proc. 38 (2021) 2555–2562. https://doi.org/10.1016/J.MATPR.2020.07.561.
30. M. Malika, R. Bhad, S.S. Sonawane, ANSYS simulation study of a low volume fraction CuO–ZnO/water hybrid nanofluid in a shell and tube heat exchanger, Journal of the Indian Chemical Society. 98 (2021) 100200. https://doi.org/10.1016/J.JICS.2021.100200.
31. M. Bhola, S. Singh, Analysis of heat transfer of turbulent channel using different geometries using ANSYS, Mater Today Proc. 64 (2022) 1223–1228. https://doi.org/10.1016/J.MATPR.2022.03.701.
32. L. Dong, W. Li, Q. Xu, J. Gu, Z. Kang, J. Chen, X. Xu, X. Zhang, X. Zhang, H. Jiang, M. Guan, A rapid multiplex assay of human malaria parasites by digital PCR, Clinica Chimica Acta. 539 (2023) 70–78. https://doi.org/10.1016/J.CCA.2022.12.001.
33. C. Costales, M.J. Broadhurst, I. Budvytiene, N. Banaei, Clinical accuracy of malaria loop-mediated isothermal amplification assay as a stand-alone screening tool at a non-endemic Northern California regional health system, Diagn Microbiol Infect Dis. 103 (2022) 115680. https://doi.org/10.1016/J.DIAGMICROBIO.2022.115680.
34. H. Pian, M. Yang, X. Sun, Z. Zheng, Sandwich hybridization-based loop-mediated isothermal amplification (SHB-LAMP) for high-throughput detection of malaria RNA from asymptomatic infections, Sens Actuators B Chem. 365 (2022) 131973. https://doi.org/10.1016/J.SNB.2022.131973.
35. L.P.Y. Zen, M.Y. Lai, S. Izzati binti Rozlan, M.H. Abdul Hamid, J. Jelip, R. Nani Mudin, Y.L. Lau, End-point detection of loop-mediated isothermal amplification (LAMP) on malaria by direct observation with colorimetric dyes, Exp Parasitol. 239 (2022) 108310. https://doi.org/10.1016/J.EXPPARA.2022.108310.
36. S. Picot, M. Cucherat, A.L. Bienvenu, Systematic review and meta-analysis of diagnostic accuracy of loop-mediated isothermal amplification (LAMP) methods compared with microscopy, polymerase chain

reaction and rapid diagnostic tests for malaria diagnosis, International Journal of Infectious Diseases. 98 (2020) 408–419. https://doi.org/10.1016/J.IJID.2020.07.009.

37. R. Struijk, A. van den Ouden, J. Louwerse, K. Čurová, R. Burggrave, B. McNally, T. de Groot, B. Mulder, G. de Vos, Ultrafast RNA extraction-free SARS-CoV-2 detection by direct RT-PCR using a rapid thermal cycling approach, Diagn Microbiol Infect Dis. 107 (2023) 115975. https://doi.org/10.1016/J.DIAGMICROBIO.2023.115975.
38. J.K. Brons, S.N. Vink, M.G.J. de Vos, S. Reuter, U. Dobrindt, J.D. van Elsas, Fast identification of Escherichia coli in urinary tract infections using a virulence gene based PCR approach in a novel thermal cycler, J Microbiol Methods. 169 (2020) 105799. https://doi.org/10.1016/J.MIMET.2019.105799.
39. M. Zhang, C. Liu, Y. Shi, J. Wu, J. Wu, H. Chen, Selective endpoint visualized detection of Vibrio parahaemolyticus with CRISPR/Cas12a assisted PCR using thermal cycler for on-site application, Talanta. 214 (2020) 120818. https://doi.org/10.1016/J.TALANTA.2020.120818.
40. Y. kun Lou, H. Qin, E. Molodysky, B.J. Morris, Simple microwave and thermal cycler boiling methods for preparation of cervicovaginal lavage cell samples prior to PCR for human papillomavirus detection, J Virol Methods. 44 (1993) 77–81. https://doi.org/10.1016/0166-0934(93)90009-G.
41. M.R. Uribe, S. Adams, K. Barracchini, J. Hackett, F. Marincola, D. Stroncek, An alternative PCR-based method for monitoring thermal cycler performance, Hum Immunol. 64 (2003) S177. https://doi.org/10.1016/J.HUMIMM.2003.08.338.
42. J. Nabuti, A.R. Fath Elbab, A. Abdel-Mawgood, M. Yoshihisa, H.M.H. Shalaby, Highly efficient photonic PCR system based on plasmonic heating of gold nanofilms, Biosens Bioelectron X. 14 (2023) 100346. https://doi.org/10.1016/J.BIOSX.2023.100346.
43. T. Higashi, H. Minegishi, A. Echigo, Y. Nagaoka, T. Fukuda, R. Usami, T. Maekawa, T. Hanajiri, Nanomaterial-assisted PCR based on thermal generation from magnetic nanoparticles under high-frequency AC magnetic fields, Chem Phys Lett. 635 (2015) 234–240. https://doi.org/10.1016/J.CPLETT.2015.06.070.
44. B.E. Gama, F. do E.S. Silva-Pires, M.N.K.R. Lopes, M.A.B. Cardoso, C. Britto, K.L. Torres, L. de Mendonça Lima, J.M. de Souza, C.T. Daniel-Ribeiro, M. de Fátima Ferreira-da-Cruz, Real-time PCR versus conventional PCR for malaria parasite detection in low-grade parasitemia, Exp Parasitol. 116 (2007) 427–432. https://doi.org/10.1016/J.EXPPARA.2007.02.011.
45. M.J. Godin, A. Sebastian, I. Albert, S.E. Lindner, Long-read genome assembly and gene model annotations for the rodent malaria parasite Plasmodium yoelii 17XNL, Journal of Biological Chemistry. 299 (2023) 104871. https://doi.org/10.1016/J.JBC.2023.104871.
46. Y. Cao, C. Ye, C. Zhang, G. Zhang, H. Hu, Z. Zhang, H. Fang, J. Zheng, H. Liu, Simultaneous detection of multiple foodborne bacteria by loop-mediated isothermal amplification on a microfluidic chip through colorimetric and fluorescent assay, Food Control. 134 (2022) 108694. https://doi.org/10.1016/J.FOODCONT.2021.108694.
47. X. Cao, S. Ge, X. Zhou, Y. Mao, Y. Sun, W. Lu, M. Ran, A dual-signal amplification strategy based on pump-free SERS microfluidic chip for rapid and ultrasensitive detection of non-small cell lung cancer-related circulating tumour DNA in mice serum, Biosens Bioelectron. 205 (2022) 114110. https://doi.org/10.1016/J.BIOS.2022.114110.
48. Z. Zhou, X. Lan, L. Zhu, Y. Zhang, K. Chen, W. Zhang, W. Xu, Portable dual-aptamer microfluidic chip biosensor for Bacillus cereus based on aptamer tailoring and dumbbell-shaped probes, J Hazard Mater. 445 (2023) 130545. https://doi.org/10.1016/J.JHAZMAT.2022.130545.
49. Z. Gao, L. Jin, C. Jia, X. Wang, J. Zhao, S. Feng, X. Guo, A droplet digital PCR chip with passive bubble removal for absolute nucleic acid quantification, Sens Actuators B Chem. 392 (2023) 134109. https://doi.org/10.1016/J.SNB.2023.134109.
50. W. Su, J. Qiu, Y. Mei, X.E. Zhang, Y. He, F. Li, A microfluidic cell chip for virus isolation via rapid screening for permissive cells, Virol Sin. 37 (2022) 547–557. https://doi.org/10.1016/J.VIRS.2022.04.011.
51. Y. Lu, Z. Tong, Z. Wu, X. Jian, L. Zhou, S. Qiu, C. Shen, H. Yin, H. Mao, Multiple exosome RNA analysis methods for lung cancer diagnosis through integrated on-chip microfluidic system, Chinese Chemical Letters. 33 (2022) 3188–3192. https://doi.org/10.1016/J.CCLET.2021.12.045.
52. E. Kim, G.Y. Lee, S.M. Yang, H.Y. Kim, Rapid and accurate on-site identification of Lactobacillus delbrueckii subspecies in dairy products using direct polymerase chain reaction with microfluidic chip, LWT. 179 (2023) 114635. https://doi.org/10.1016/J.LWT.2023.114635.
53. C. Wu, L. Liu, Z. Ye, J. Gong, P. Hao, J. Ping, Y. Ying, TriD-LAMP: A pump-free microfluidic chip for duplex droplet digital loop-mediated isothermal amplification analysis, Anal Chim Acta. 1233 (2022) 340513. https://doi.org/10.1016/J.ACA.2022.340513.
54. F. Parvizi, A. Parvareh, R. Heydari, Fabrication of a hydrophobic surface as a new supported liquid membrane for microfluidic based liquid phase microextraction device using modified boehmite nanoparticles (AlOO-NSPO), Microchemical Journal. 189 (2023) 108514. https://doi.org/10.1016/J.MICROC.2023.108514.

55. F. Zarghampour, Y. Yamini, E. Alipanahpour Dil, A. Shokrollahi, G. Javadian, A new microfluidic-chip device followed by sensitive image analysis of smart phone for simultaneous determination of dyes with different acidic–basic properties, Talanta. 254 (2023) 124168. https://doi.org/10.1016/J.TALANTA.2022.124168.
56. D. Zhang, R. Gao, S. Huang, Y. Huang, J. Zhang, X. Su, S. Zhang, S. Ge, J. Zhang, N. Xia, All-in-one microfluidic chip for 30-min quantitative point-of-care-testing of nucleic acids, Sens Actuators B Chem. 390 (2023) 133939. https://doi.org/10.1016/J.SNB.2023.133939.
57. K. Yang, J. Pan, G. Deng, C. Hua, C. Zhu, Y. Liu, L. Zhu, Mkit: A mobile nucleic acid assay based on a chitosan-modified minimalistic microfluidic chip (CM3-chip) and smartphone, Anal Chim Acta. 1253 (2023) 341030. https://doi.org/10.1016/J.ACA.2023.341030.
58. A.M. Kaba, H. Jeon, A. Park, K. Yi, S. Baek, A. Park, D. Kim, Cavitation-microstreaming-based lysis and DNA extraction using a laser-machined polycarbonate microfluidic chip, Sens Actuators B Chem. 346 (2021) 130511. https://doi.org/10.1016/J.SNB.2021.130511.
59. S. Su, G. Jing, M. Zhang, B. Liu, X. Zhu, B. Wang, M. Fu, L. Zhu, J. Cheng, Y. Guo, One-step bonding and hydrophobic surface modification method for rapid fabrication of polycarbonate-based droplet microfluidic chips, Sens Actuators B Chem. 282 (2019) 60–68. https://doi.org/10.1016/J.SNB.2018.11.035.
60. Y. Wang, Q. He, Y. Dong, H. Chen, In-channel modification of biosensor electrodes integrated on a polycarbonate microfluidic chip for micro flow-injection amperometric determination of glucose, Sens Actuators B Chem. 145 (2010) 553–560. https://doi.org/10.1016/J.SNB.2009.11.068.
61. W. Bi, S. Cai, T. Lei, L. Wang, Implementation of blood-brain barrier on microfluidic chip: Recent advance and future prospects, Ageing Res Rev. 87 (2023) 101921. https://doi.org/10.1016/J.ARR.2023.101921.
62. D. Zhang, R. Gao, S. Huang, Y. Huang, J. Zhang, X. Su, S. Zhang, S. Ge, J. Zhang, N. Xia, All-in-one microfluidic chip for 30-min quantitative point-of-care-testing of nucleic acids, Sens Actuators B Chem. 390 (2023) 133939. https://doi.org/10.1016/J.SNB.2023.133939.
63. H.N. Açıkgöz, A. Karaman, M.A. Şahin, Ö.R. Çaylan, G.C. Büke, E. Yıldırım, İ.C. Eroğlu, A.E. Erson-Bensan, B. Çetin, M.B. Özer, Assessment of silicon, glass, FR4, PDMS and PMMA as a chip material for acoustic particle/cell manipulation in microfluidics, Ultrasonics. 129 (2023) 106911. https://doi.org/10.1016/J.ULTRAS.2022.106911.
64. M.T. Guler, Fabricating plasma bonded microfluidic chips by CO2 laser machining of PDMS by the application of viscoelastic particle focusing and droplet generation, J Manuf Process. 73 (2022) 260–268. https://doi.org/10.1016/J.JMAPRO.2021.11.016.
65. B. Jiang, H. Guo, D. Chen, M. Zhou, Microscale investigation on the wettability and bonding mechanism of oxygen plasma-treated PDMS microfluidic chip, Appl Surf Sci. 574 (2022) 151704. https://doi.org/10.1016/J.APSUSC.2021.151704.
66. Q. Tang, X. Li, C. Lai, L. Li, H. Wu, Y. Wang, X. Shi, Fabrication of a hydroxyapatite-PDMS microfluidic chip for bone-related cell culture and drug screening, Bioact Mater. 6 (2021) 169–178. https://doi.org/10.1016/J.BIOACTMAT.2020.07.016.
67. X. Liu, S. Li, Fabrication of a Three-Layer PDMS Pneumatic Microfluidic Chip for Micro Liquid Sample Operation, SLAS Technol. 25 (2020) 151–161. https://doi.org/10.1177/2472630319870126.
68. Q. Song, J. Sun, Y. Mu, Y. Xu, Q. Zhu, Q. Jin, A new method for polydimethylsiloxane (PDMS) microfluidic chips to maintain vacuum-driven power using Parylene C, Sens Actuators B Chem. 256 (2018) 1122–1130. https://doi.org/10.1016/J.SNB.2017.10.006.
69. S.Y. Lee, J.H. Kim, S.W. Oh, Combination of filtration and immunomagnetic separation based on real-time PCR to detect foodborne pathogens in fresh-cut apple, J Microbiol Methods. 201 (2022) 106577. https://doi.org/10.1016/J.MIMET.2022.106577.
70. H.J. Lee, S. Choi, I.S. Cho, J.Y. Yoon, R.D. Jeong, Development and application of a reverse transcription droplet digital PCR assay for detection and quantification of Plantago asiatica mosaic virus, Crop Protection. 169 (2023) 106255. https://doi.org/10.1016/J.CROPRO.2023.106255.
71. P. Kheiroddin, V.D. Gaertner, P. Schöberl, E. Fischer, J. Niggel, P. Pagel, B.M.J. Lampl, A. Ambrosch, M. Kabesch, Gargle pool PCR testing in a hospital during medium and high SARS-CoV-2 incidence, Journal of Hospital Infection. 127 (2022) 69–76. https://doi.org/10.1016/J.JHIN.2022.05.018.
72. N. Guan, Y. Li, H. Yang, P. Hu, S. Lu, H. Ren, Z. Liu, K. Soo Park, Y. Zhou, Dual-functionalized gold nanoparticles probe based bio-barcode immuno-PCR for the detection of glyphosate, Food Chem. 338 (2021) 128133. https://doi.org/10.1016/J.FOODCHEM.2020.128133.

73. J.A. Huber, H.G. Morrison, S.M. Huse, P.R. Neal, M.L. Sogin, D.B. Mark Welch, Effect of PCR amplicon size on assessments of clone library microbial diversity and community structure, Environ Microbiol. 11 (2009) 1292. https://doi.org/10.1111/J.1462-2920.2008.01857.X.
74. N. Hofmann, F. Mwingira, S. Shekalaghe, L.J. Robinson, I. Mueller, I. Felger, Ultra-Sensitive Detection of Plasmodium falciparum by Amplification of Multi-Copy Subtelomeric Targets, PLoS Med. 12 (2015) e1001788. https://doi.org/10.1371/JOURNAL.PMED.1001788.